Published in final edited form as:
Microcirculation. 2009 October ; 16(7): 603–614. doi:10.1080/10739680903114268.

Rat Strain Differences in Pulmonary Artery Smooth Muscle Ca^{2+} Entry Following Chronic Hypoxia

JESSICA B. SNOW, **NANCY L. KANAGY**, **BENJIMEN R. WALKER**, and **THOMAS C. RESTA**
Vascular Physiology Group, Department of Cell Biology and Physiology, University of New Mexico Health Sciences Center, Albuquerque, New Mexico, USA

Abstract

Effects of chronic hypoxia (CH) on store- and receptor-operated Ca^{2+} entry (SOCE, ROCE) in pulmonary vascular smooth muscle (VSM) are controversial, although whether genetic variation explains such discrepancies in commonly studied rat strains is unclear. Since protein kinase C (PKC) can inhibit Ca^{2+} permeable nonselective cation channels, we hypothesized that CH differentially alters PKC-dependent inhibition of SOCE and ROCE in pulmonary VSM from Sprague-Dawley and Wistar rats. To test this hypothesis, we examined SOCE and endothelin-1 (ET-1)-induced ROCE in endothelium-disrupted, pressurized pulmonary arteries from control and CH Sprague-Dawley and Wistar rats. Basal VSM Ca^{2+} was elevated in CH Wistar, but not Sprague-Dawley, rats. Further, CH attenuated SOCE in VSM from Sprague-Dawley rats, while augmenting this response in Wistar rats. CH reduced ROCE in arteries from both strains. PKC inhibition restored SOCE in CH Sprague-Dawley arteries to control levels, while having no effect on SOCE in Wistar arteries or on ROCE in either strain. We conclude that effects of CH on pulmonary VSM SOCE are strain dependent, whereas inhibitory effects of CH on ROCE are strain independent. Further, PKC inhibits SOCE following CH in Sprague-Dawley, but not Wistar, rats but does not contribute to ET-1-induced ROCE in either strain.

Keywords

pulmonary hypertension; endothelin-1; store-operated Ca^{2+} entry; receptor-operated Ca^{2+} entry; vasoconstriction; Sprague-Dawley; Wistar

Chronic hypoxia (CH), resulting from residence at high altitude or chronic obstructive lung disease, increases pulmonary vascular resistance, leading to pulmonary hypertension. The severity of the resulting pulmonary hypertension depends, in part, on the vascular smooth muscle (VSM) cytosolic free Ca^{2+} concentration ($[Ca^{2+}]_i$), which mediates both vaso-constriction and arterial hypertrophy [8,35,44,45,47]. Many endogenous agonists that contribute to CH-induced pulmonary hypertension, such as endothelin-1 (ET-1) [4], serotonin [10], and thromboxanes [18], are thought to activate both store- and receptor-operated channels (SOC, ROC) in VSM, leading to elevated $[Ca^{2+}]_i$ [16,17,48].

Store-operated Ca^{2+} entry (SOCE) is a highly conserved cellular mechanism, by which the depletion of intracellular Ca^{2+} stores activates cation influx through voltage-independent, nonselective cation channels [25,33,37,40]. An additional mechanism of Ca^{2+} influx, termed receptor-operated Ca^{2+} entry (ROCE), involves the stimulation of similar nonselective

Address correspondence to Jessica B. Snow, Department of Cell Biology and Physiology, University of New Mexico Health Sciences Center, MSC 08-4750, 1 University of New Mexico, Albuquerque, NM 87131-0001, USA. jsnow@salud.unm.edu.

Declaration of interest: The authors report no financial conflicts of interest. The authors alone are responsible for the content and writing of this paper.

cation channels by diacylglycerol (DAG) [9,11], a second messenger produced following receptor stimulation and resultant phospholipase C/D (PLC/D) activation. Basal activity, as well as agonist-mediated activation of these channels, may contribute to altered pulmonary VSM Ca^{2+} homeostasis in pulmonary hypertension. Interestingly, variable effects of CH have been reported not only with respect to basal pulmonary VSM $[Ca^{2+}]_i$ [12,14,22,35], but to Ca^{2+} entry mechanisms as well [12,22,41]. However, whether such divergent responses to CH represent phenotypic differences between the Sprague-Dawley and Wistar rat strains commonly used in CH studies has not been addressed. The aim of the present study was to determine whether SOCE and ROCE are differentially regulated by CH between these two rat strains and to further examine potential signaling mechanisms responsible for such contrasting effects of CH on VSM Ca^{2+} homeostasis in Sprague-Dawley and Wistar rats.

The most widely studied candidates for SOC and ROC are the canonical transient receptor potential (TRPC) family of nonselective cation channels [22,40]. Because protein kinase C (PKC) activation has been implicated in the negative regulation of TRPC channels in HEK293 and DT40 cells [39], we hypothesized that CH differentially alters PKC-dependent inhibition of SOCE and ROCE in pulmonary VSM between Sprague-Dawley and Wistar rats. Our data indicate that PKC attenuates SOCE in pulmonary VSM from CH Sprague-Dawley rats. However, CH-augmented SOCE in arteries from Wistar rats through a mechanism independent of PKC. Further, ET-1-induced ROCE was attenuated following CH in both strains of rats, a response that was unaltered by PKC inhibition.

METHODS

All protocols and surgical procedures employed in this study were reviewed and approved by the Institutional Animal Care and Use Committee of the University of New Mexico Health Sciences Center (Albuquerque, New Mexico, USA). Animals were maintained on a 12-hour light-dark cycle.

Chronic Hypoxic Exposure

Male Sprague-Dawley and Wistar rats (240–350 g body weight on the day of experimentation; Harlan Industries, Indianapolis, USA) were divided into two groups. Animals designated for exposure to CH were housed in a hypobaric chamber with barometric pressure maintained at ~380 mmHg for four weeks. The chamber was opened three times per week to provide animals with fresh food, water, and clean bedding. On the day of experimentation, rats were removed from the hypobaric chamber and immediately placed in Plexiglas chambers continuously flushed with a 12% O_2–88% N_2 gas mixture to reproduce inspired Po_2 (~70 mmHg) within the hypobaric chamber. Control animals were housed at ambient barometric pressure (~630 mmHg).

Assessment of Hematocrit and Right Ventricular Weight

Blood samples were obtained by direct cardiac puncture at the time of lung isolation for the measurement of hematocrit. Right ventricular hypertrophy was assessed as an index of pulmonary hypertension, as previously described [30,32]. Briefly, after isolation of the heart, the atria and major vessels were removed from the ventricles. The right ventricle (RV) was dissected from the left ventricle and septum (LV+S), and each was cleaned of blood and weighed. The degree of right ventricular hypertrophy was expressed as the ratio of RV to total ventricle weight (T) and as the ratio of RV to body weight.

Isolation of Small Pulmonary Arteries for Dimensional Analysis

Rats were anesthetized with pentobarbital sodium (200 mg/kg intraperitoneally), and the heart and lungs were exposed by midline thoracotomy. The left lung was removed and

immediately placed in ice-cold physiological salt solution [(PSS) containing (in mM): 129.8 NaCl, 5.4 KCl, 0.5 NaH_2PO_4, 0.83 $MgSO_4$, 10 $NaHCO_3$, 1.8 $CaCl_2$, and 5.5 glucose]. A fourth- or fifth-order intrapulmonary artery [~100–200 μm inner diameter (ID)] of ~1 mm length and without side branches was dissected free and transferred to a vessel chamber (CH-1; Living Systems, Burlington, VT, USA) containing ice-cold PSS. The proximal end of the artery was cannulated with a tapered glass pipette, secured in place with a single strand of silk ligature, and gently flushed to remove any blood from the lumen. Before cannulation of the distal end of the artery, a strand of moose mane (commercially available from fishing supply retailers) was passed through the lumen to disrupt the endothelium. The vessel was then stretched longitudinally to approximate its *in situ* length and pressurized with a servo-controlled peristaltic pump (Living Systems) to 12 mmHg. The absence of leaks was determined by turning off the servo-control function and observing the maintenance of pressure. Any vessels with apparent leaks were discarded. The vessel chamber was transferred to the stage of a Nikon Eclipse TS100 microscope (Melville, NY, USA), and the preparation was superfused with PSS equilibrated with a 10% O_2, 6% CO_2, and balance N_2 gas mixture. A vessel chamber cover was positioned to allow this same gas mixture to flow over the top of the chamber bath. Bright-field images of vessels were obtained with an IonOptix CCD100M camera, (Milton, MA, USA) and dimensional analysis was performed by IonOptix Sarclen software to measure ID. Experiments were conducted at a bath temperature of 37°C. The effectiveness of endothelial disruption was verified by the lack of a vasodilatory response to acetylcholine (ACh) (1 μM) in uridine triphosphate (UTP) (5 μM)-constricted vessels, as previously reported [3,12–14].

Measurement of VSM $[Ca^{2+}]_i$

Pressurized arteries were loaded abluminally with the cell-permeant, ratiometric, Ca^{2+}-sensitive fluorescent indicator, fura-2 AM (Molecular Probes, Carlsbad, CA, USA), as described previously [3,12–14]. Immediately before being loaded, fura-2 AM (1 mM in anhydrous dimethyl sulfoxide; DMSO) was mixed (2:1) with a 20% solution of pluronic acid in DMSO, and this mixture was diluted in PSS to yield a final concentration of 2-μM fura-2 AM and 0.05% pluronic acid. Arteries were incubated in this solution for 45 minutes at room temperature (~25°C) in the dark. The diluted fura-2 AM solution was equilibrated with the 10% O_2 gas mixture during this loading period. Vessels were then rinsed for 20 minutes with aerated PSS (37°C) to wash out excess dye and to allow for the hydrolysis of AM groups by intracellular esterases. Fura-2-loaded vessels were alternately excited at 340 and 380 nm with an IonOptix Hyperswitch dual-excitation light source, and the respective 510-nm emissions were collected with a photomultiplier tube. Background-subtracted 340/380 emission ratios were calculated with IonOptix Ion Wizard software and recorded continuously throughout the experiment, with the simultaneous measurement of ID from red wavelength bright-field images, as described above.

In Situ Calibrations of VSM $[Ca^{2+}]_i$

In situ calibrations for Ca^{2+} were performed in pressurized arteries from control and CH Sprague-Dawley and Wistar rats, using methods similar to those previously described [19]. Arteries were loaded with fura-2 AM and prepared for experimentation, as described above. The VSM was then permeabilized to Ca^{2+} with ionomycin (10μM). and the arteries were incubated with a bath solution containing 140 mM KCl, 5 mM NaCl, 5 mM HEPES, 1 mM $MgCl_2$, 5 μM nigericin, and either 5 mM ethylene glycol tetraacetic acid (EGTA) (low Ca^{2+} solution), solution) or 2 mM $CaCl_2$ (high Ca^{2+} with a pH of 7.15 at 37°C until nadir and peak ratios were achieved.

Isolated Vessel Protocols

Because the endothelium is a source of vasoactive factors that may complicate the interpretation of the effects of CH on VSM Ca^{2+} entry mechanisms, all experiments were conducted in endothelium-disrupted arteries.

Contribution of PKC to Altered SOCE following CH

After fura-2 AM loading, pulmonary arteries from control and CH rats of each strain were equilibrated with PSS containing diltiazem (50 μM; Sigma) to inhibit Ca^{2+} entry through L-type voltage-gated Ca^{2+} channels, and superfused with Ca^{2+}-free PSS containing 3 mM EGTA to chelate any residual Ca^{2+}. We have previously shown that this concentration of diltiazem inhibits depolarization-induced increases in VSM $[Ca^{2+}]_i$ in this preparation [12]. In addition, arteries were incubated with the sarcoplasmic reticulum Ca^{2+}-ATPase (SERCA) inhibitor, cyclopiazonic acid (CPA; 10 μM; Sigma), to deplete intracellular Ca^{2+} stores and prevent Ca^{2+} reuptake. This concentration of CPA has been shown to effectively deplete SR calcium stores in this preparation [12]. Vessels were superfused with Ca^{2+}-free PSS containing diltiazem for five minutes, followed by 10 minutes of exposure to the same solution with the addition of CPA. The changes in $[Ca^{2+}]_i$ (SOCE) and ID were then determined upon the restoration of extracellular Ca^{2+} (1.8 mM) in the continued presence of diltiazem and CPA [12]. To assess the role of PKC in regulating SOCE, separate sets of vessels were pretreated with the general PKC inhibitor, GF109203X (1 μM; Biomol, Plymouth Meeting, PA, USA), and CPA-induced SOCE and vasoconstriction were evaluated, as described above. This concentration of GF109203X inhibits PKC-dependent vasoconstriction in this preparation [3,12,13].

Role of PKC in Altered ROCE following CH

To evaluate possible strain differences in the effects of CH on ROCE, the vasoconstrictor peptide, ET-1, was used to induce ROCE similar to that previously described [12]. To assess ROCE independently of SOCE and to eliminate other ET-1-mediated Ca^{2+} entry mechanisms, vessels were pretreated with diltiazem (50 μM) and CPA (10 μM), and a stable SOCE response was obtained (described above) before the addition of ET-1 (10^{-9}–10^{-7} M; Sigma, St. Louis, MO, USA). Similar experiments were performed in the presence of GF109203X (1 μM) to assess the contribution of PKC to ET-1-induced ROCE.

Calculations and Statistical Analysis

In SOCE experiments, vasoconstrictor responses were calculated as a percent of baseline ID. In ROCE experiments, vasoconstrictor responses were calculated as a percent of ID at the plateau of the SOCE response. VSM $[Ca^{2+}]_i$ is expressed as the background-subtracted ratios of fluorescence (F) emitted following excitation at 340 and 380 nm (F_{340}/F_{380}). All data are expressed as means±standard error of the mean, and values of *n* refer to the number of animals in each group. A *t*-test, one-way analysis of variance (ANOVA), or two-way ANOVA was used to make comparisons, when appropriate. If differences were detected by ANOVA, individual groups were compared with the Student-Newman-Keuls test. A probability of $P < 0.05$ was accepted as significant for all comparisons.

RESULTS

Polycythemia

Both Sprague-Dawley and Wistar rats exhibited CH-induced polycythemia, as indicated by greater hematocrit, compared with normoxic control rats (Figure 1A). Furthermore, CH elicited a significantly greater polycythemic response in Wistar, compared to Sprague-Dawley rats.

Right Ventricular Hypertrophy

Ratios of right ventricle weight to body weight (RV/BW) were increased by CH in both rat strains (Figure 1B), thus demonstrating right ventricular hypertrophy indicative of pulmonary hypertension. No differences in RV/BW were observed between Sprague-Dawley and Wistar control rats. However, similar to strain differences in hematocrit (Figure 1A), Wistar rats demonstrated significantly greater RV/BW following CH, compared to Sprague-Dawley rats (Figure 1B), suggestive of greater CH-induced pulmonary hypertension in the Wistar strain. Ratios of right ventricle weight to total heart weight (RV/T) were also increased by CH in rats from both groups (Table 1). Ratios of left ventricle plus septum to body weight (LV+S/BW) were greater in CH Wistar than control Wistar rats, although a similar relationship was not observed in the Sprague-Dawley strain. Body weight was greater in control Wistar, compared to control Sprague-Dawley, rats, although no differences in body weight were observed between strains following exposure to CH (Table 1).

In Situ Calibrations of VSM $[Ca^{2+}]_i$

Comparisons of *in situ* calibration values in pressurized small pulmonary arteries revealed no significant differences between vessels from control or CH, Sprague-Dawley, or Wistar rats (Table 2), suggesting that fura-2 displays similar kinetics in VSM between groups. Consequently, all VSM $[Ca^{2+}]_i$ data are expressed as fura-2 ratios.

Basal VSM $[Ca^{2+}]_i$

Basal VSM $[Ca^{2+}]_i$ was not significantly different between control and CH Sprague-Dawley rats (Figure 2). In contrast, CH increased basal VSM $[Ca^{2+}]_i$ in arteries from Wistar rats, in agreement with previous studies [36,41]. Intralumenal diameters for control and CH Sprague-Dawley and Wistar rats are shown in Table 3.

Store-operated Ca^{2+} Entry

To assess influences of CH and PKC on SOCE, the SERCA inhibitor, CPA, was used to deplete SR stores and thereby activate store-operated channels, whereas diltiazem was present to eliminate Ca^{2+} influx through L-type voltage-gated Ca^{2+} channels. Figure 3 depicts a trace of VSM $[Ca^{2+}]_i$ in which both SOCE and ET-1-induced ROCE were evaluated in a pulmonary artery from a control rat.

Sprague-Dawley—CH diminished SOCE in pulmonary VSM from Sprague-Dawley rats (Figure 4A). The vasoconstriction associated with CPA-induced SOCE was similarly attenuated following CH (Figure 4B). The broad-spectrum PKC inhibitor, GF109203X (1 μM), restored SOCE in arteries from CH Sprague-Dawley rats to the level of controls (Figure 4A), suggesting an inhibitory effect of PKC on SOCE in the setting of CH. Although PKC inhibition was without effect on SOCE in control Sprague-Dawley rats, GF109203X significantly reduced the associated vasoconstriction, thus supporting a role for PKC to mediate SOCE-induced vasoconstriction through a VSM Ca^{2+} sensitization mechanism.

Wistar—In contrast to inhibitory effects of CH on SOCE in arteries from Sprague-Dawley rats (Figure 4A), SOCE was augmented following CH in vessels from Wistar rats (Figure 5A). Furthermore, PKC inhibition had no effect on SOCE (Figure 5A) or associated constriction (Figure 5B) in arteries from either control or CH Wistar rats.

ET-1–induced Receptor-operated Ca^{2+} Entry

Sprague-Dawley—ET-1–induced ROCE was diminished following CH in arteries from Sprague-Dawley rats (Figure 6A), as previously reported for UTP-induced ROCE [12]. In

contrast to effects of PKC inhibition on SOCE (Figure 4A), GF109203X had no effect on ET-1-induced ROCE in vessels from either control or CH Sprague-Dawley rats (Figure 6A). Despite the marked reduction in ROCE following CH, ET-1-mediated vasoconstrictor responses were similar between groups, thus supporting recent findings that CH augments ET-1-induced pulmonary VSM Ca^{2+}-sensitization [15]. Furthermore, GF109203X attenuated the vasoconstriction associated with ET-1 (10 nM)-induced ROCE in arteries from CH Sprague-Dawley rats (Figure 6B), indicating a contribution of PKC to this response.

Wistar—Similar to the inhibitory effect of CH on ROCE in arteries from Sprague-Dawley rats, ET-1-induced ROCE tended to be decreased in pulmonary VSM from CH Wistar rats, compared to controls, although significance was achieved only in GF109203X-pretreated vessels (Figure 7A). In addition, GF109203X was without effect on ROCE in arteries from either control or CH Wistar rats. Vasoconstrictor responses associated with ET-1-induced ROCE were not different between control and CH vehicle groups in either rat strain. However, as in vessels from Sprague-Dawley rats (Figure 6B), GF109203X significantly attenuated the vasoconstriction to ET-1 (1 and 10 nM) in arteries from CH Wistar rats (Figure 7B).

DISCUSSION

The present study tested the hypothesis that CH differentially alters PKC-dependent inhibition of SOCE and ROCE in pulmonary VSM from Sprague-Dawley and Wistar rats. The major findings from this study are that: 1) Wistar rats developed greater polycythemia and right ventricular hypertrophy following CH than Sprague-Dawley rats; 2) CH increased basal VSM $[Ca^{2+}]_i$ in small pulmonary arteries from Wistar rats, but was without effect on basal VSM $[Ca^{2+}]_i$ in Sprague-Dawley rats; 3) pulmonary VSM SOCE was augmented in CH Wistar rats, compared to control animals, whereas CH decreased SOCE in arteries from Sprague-Dawley rats; 4) PKC contributed to reduced SOCE in vessels from CH Sprague-Dawley rats, although a similar regulatory effect of PKC was not observed in arteries from Wistar rats; and 5) CH decreased ET-1-induced ROCE in pulmonary VSM from both Sprague-Dawley and Wistar rats through a PKC-independent mechanism. These results demonstrate a role for genetic variation in the effects of CH on pulmonary VSM Ca^{2+} mobilization, polycythemia, and right ventricular hypertrophy. Additionally, the data indicate a novel effect of PKC to inhibit SOCE in the hypertensive pulmonary circulation of Sprague-Dawley rats.

In agreement with previous studies [31], our current findings indicate that Wistar rats develop greater polycythemia and right ventricular hypertrophy than Sprague-Dawley rats in response to CH. The mechanism of this differential responsiveness to CH between Wistar and Sprague-Dawley remains to be determined, but may result from differences in hypoxic ventilatory responsiveness, renal-tissue oxygenation, hypoxia-inducible gene expression, rate of development of pulmonary hypertension, pulmonary vasoreactivity, or synthesis of vasoactive or growth factors that contribute to arterial constrictor and remodeling components of pulmonary hypertension. Similar differences in susceptibility to hypoxic pulmonary hypertension between rat strains have been observed by Zhao and colleagues [49], who reported that three-week hypoxic exposure elicits a greater increase in pulmonary artery pressure and right ventricular hypertrophy in Wistar Kyoto, compared to Fisher, rats. Further, the Hilltop strain of Sprague-Dawley rat demonstrates exaggerated responses to CH, compared to the Madison strain, including more severe pulmonary hypertension, arterial remodeling, and polycythemia [21,28], perhaps as a result of greater hypoxia inducible factor-1 activity [6]. Genetic predisposition to hypoxic pulmonary hypertension has also been reported in human residents of high altitude exposed to ambient hypoxia [26].

In addition, recent studies have identified heterozygous germ-line mutations in bone morphogenic protein receptor (BMPR) in patients with primary pulmonary hypertension, indicative of a genetic susceptibility to the development of pulmonary hypertension [5,24].

Previous findings, that basal VSM $[Ca^{2+}]_i$ is not different between control and CH Sprague-Dawley rats [12,13], are at odds with reports indicating that CH increases resting $[Ca^{2+}]_i$ in mice and Wistar rats [22,35,41]. However, whether such discrepant findings relate to the various preparations employed or to strain/species differences is not clear. To directly address a potential role for rat-strain differences in mediating these discrepant results, we performed parallel experiments in isolated pulmonary arteries from Sprague-Dawley and Wistar rats following exposure to four weeks of hypobaric hypoxia to examine the effect of CH on basal VSM $[Ca^{2+}]_i$. Whereas no differences in basal VSM $[Ca^{2+}]_i$ were observed after CH in Sprague-Dawley rats, CH was associated with an increase in VSM $[Ca^{2+}]_i$ in Wistar rats. Similar to this effect of CH on basal VSM $[Ca^{2+}]_i$ in Wistar rats, we have presently observed enhanced VSM SOCE following CH in isolated pulmonary arteries from this strain. These findings are consistent with earlier studies using acutely cultured pulmonary arterial myocytes from CH Wistar rats and mice [35,41], as well as in VSM from patients with idiopathic pulmonary hypertension [46]. In contrast, CH had the opposite effect of reducing SOCE in arteries from Sprague-Dawley rats, thus resolving previous discrepancies in the literature and demonstrating marked strain differences in CH-induced alterations in VSM Ca^{2+} homeostasis and SOCE. Whether such divergent effects of CH on VSM Ca^{2+} regulation contribute to the apparent differences in the degree of pulmonary hypertension between Sprague-Dawley and Wistar rats remains to be addressed.

The mechanism by which CH increases both basal $[Ca^{2+}]_i$ and SOCE in pulmonary VSM from Wistar rats and mice may involve an increase in the expression of TRPC1 channels [22], a response mediated by the transcription factor hypoxia-inducible factor (HIF)-1 [41]. While our present finding, that SOCE is attenuated following CH in Sprague-Dawley rats, could potentially be explained by a paradoxical decrease in TRPC1 expression, this is unlikely if the TRPC1 gene contains an HIF binding site [41]. Therefore, we investigated an alternative hypothesis, that PKC-mediated inhibition of SOCE is enhanced following CH in pulmonary VSM from this strain of rat. Consistent with this hypothesis, PKC inhibits the activation of various TRPC isoforms (TRPC3, −4, and −5) transfected into HEK293 and DT40 cells [39]. This inhibitory effect of PKC on the activity of TRPC channels [50] appears to be mediated, in part, by direct phosphorylation of the channel [50], although PKC also appears to inhibit TRPC3 channels in HEK cells indirectly through the stimulation of PKG [20]. Although these studies examined PKC inhibition of 1-oleoyl-2-acetyl-sn-glycerol (OAG)-induced Ca^{2+} entry, it is possible that channels mediating SOCE are similarly inhibited by PKC. This possibility is supported by our present observations that PKC inhibition augmented SOCE in vessels from CH Sprague-Dawley rats to the level of normoxic controls, thus demonstrating a novel role for PKC to regulate VSM SOCE in the hypertensive pulmonary circulation. This restoration of SOCE by PKC inhibition in CH Sprague-Dawley arteries further suggests that TRPC1 expression does not decrease. In contrast to the effect of GF109203X on SOCE in pulmonary arteries from CH Sprague-Dawley rats, PKC inhibition did not alter SOCE in CH Wistar rats, suggesting a differential effect of hypoxia on PKC expression or activity between rat strains. Such a CH-induced upregulation of PKC signaling in VSM of Sprague-Dawley rats may serve as a protective mechanism that limits the severity of pulmonary hypertension by attenuating Ca^{2+} entry.

CH may enhance the PKC-mediated inhibition of SOCE in Sprague-Dawley rats through increases in PKC activity or improved coupling of PKC to proximal or distal second-messenger molecules in microcellular signaling domains. Interestingly, intermittent hypoxia increases PKCδ activity in rat mesenteric arteries [1]. Similarly, six hours of hypoxia/

aglycemia induces a profound increase in PKCε activity in cultured bovine brain microvessel endothelial cells [43]. Hypoxia has been further shown to increase DAG levels through various mechanisms [2,38]. These elevated DAG levels are associated with greater PKC activation in VSM [7], which could account for elevated PKC-dependent SOCE inhibition following CH. Future studies are necessary to address the effect of CH on PKC expression, activity, and DAG levels in pulmonary VSM from Sprague-Dawley rats. It is alternatively possible that SOCE in Sprague-Dawley rats is mediated by a PKC-regulated cation channel(s) distinct from that responsible for SOCE in Wistar rats. Thus, different SOC channels may underlie the contrasting effects of CH on SOCE between Wistar and Sprague-Dawley strains.

Another possible explanation for the differential effects of CH on SOCE in the two rat strains involves K^+-channel expression or activity. As an important regulator of membrane potential, K^+-channels contribute to the electrical driving potential for Ca^{2+} to enter the cell. However, K^+-channel expression has been shown to be decreased by CH in pulmonary artery smooth muscle from both Sprague-Dawley and Wistar rats [29,42], leading to depolarization, which would, presumably, decrease Ca^{2+} entry. While reduced SOCE was, in fact, observed in arteries from Sprague-Dawley rats, depolarization would not be expected to account for the augmented SOCE in arteries from CH Wistar rats.

Despite the fact that PKC inhibition augmented SOCE in arteries from CH Sprague-Dawley rats, we did not observe an associated increase in vasoconstriction. This discrepancy may be explained by an effect of PKC inhibition to mask any contribution of enhanced SOCE to vasoreactivity due to inhibition of PKC-dependent Ca^{2+} sensitization.

We have previously reported that, similar to effects of CH on SOCE, UTP-induced ROCE is diminished in pulmonary VSM from Sprague-Dawley rats. In contrast, others have found that OAG-induced ROCE is augmented in isolated cells from CH Wistar rats [22]. We, therefore, hypothesized that CH differentially alters PKC-dependent inhibition of ROCE in pulmonary VSM between these two rat strains. Although CH attenuated ET-1-induced ROCE in pulmonary VSM from Sprague-Dawley rats, as predicted, we observed a similar inhibitory effect of CH on ET-1-induced ROCE in pulmonary arteries from Wistar rats. Consistent with these findings, Shimoda et al. [35] reported that CH attenuates ET-1-induced increases in $[Ca^{2+}]_i$ in PASMC from Wistar rats. One potential explanation for the different results in using receptor-mediated agonists and OAG to stimulate ROCE is that there is a diminished ability of G-protein–coupled receptors to stimulate DAG production following CH. This could be related either to reduced DAG production by PLC or PLD, or enhanced degradation by DAG kinase [27,38] and DAG lipase [34]. Directly stimulating ROCE with a DAG analog would not reveal such an aberration in the coupling of receptor stimulation to DAG synthesis. In addition, SOC and ROC are commonly thought to be composed of heterotetramers, and the subunit stoichiometry may be changed following CH, based on the finding that TRPC6 expression is increased by CH but expression of TRPC3 is not [22]. If OAG and receptor-mediated agonists stimulate different TRPC isoforms in the setting of altered channel configuration, this could explain the differing effects of CH on OAG and ET-1-induced ROCE. Finally, PLC activation and OAG can stimulate different isoforms of PKC [23], which may account for contrasting effects of OAG and ET-1 on Ca^{2+} entry. Together, these findings suggest that hypoxia differentially alters OAG-induced and receptor-mediated activation of ROC, and the effects are not strain dependent.

We observed no differences in ROCE-associated vasoconstriction between control and CH vehicle groups, despite an effect of CH to blunt ROCE, findings that are consistent with previous reports that CH enhances ET-1-induced Ca^{2+} sensitization in pulmonary VSM [3,14]. The effect of PKC inhibition to attenuate ET-1-mediated constriction in arteries from

both CH Sprague-Dawley and Wistar rats, despite similar ROCE, further supports a role for CH to augment a PKC-dependent Ca^{2+} sensitization mechanism in small pulmonary arteries.

CONCLUSIONS

In summary, the present study demonstrates contrasting effects of CH on basal VSM $[Ca^{2+}]_i$ and SOCE, but a similar reduction in ROCE in two commonly studied rat strains. In Wistar rats, CH induces more robust polycythemia and right ventricular hypertrophy, which are hallmarks of pulmonary hypertension. Given that $[Ca^{2+}]_i$ is a major stimulus for VSM contraction, proliferation, and gene expression, it is possible that increased basal VSM $[Ca^{2+}]_i$ and SOCE contribute to greater pulmonary hypertension in Wistar rats. Conversely, the diminished Ca^{2+} responses and lack of an increase in basal Ca^{2+} in Sprague-Dawley rats may serve as a protective mechanism, effectively limiting increases in vascular resistance in the setting of CH. We have further identified a novel role for PKC to inhibit SOCE in the hypertensive pulmonary circulation of Sprague-Dawley, but not Wistar, rats. Whether such differences in VSM Ca^{2+} regulation between Sprague-Dawley and Wistar rats reflect genetic differences in the expression of SOC channels, PKC, or hypoxic regulation of gene expression remains to be addressed.

Acknowledgments

The authors thank Permelia Allgood, Dr. Brad Broughton, Ph.D., Minerva Murphy, and Charles Norton for their technical assistance. This work was supported by the National Heart, Lung and Blood Institute (grants HL77876 and HL88192 to TCR; HL58124 and HL07736 to BRW) and the American Heart Association (Grant-In-Aid #0755775Z to TCR; Predoctoral Fellowship #0715682Z to JBS).

References

1. Allahdadi KJ, Duling LC, Walker BR, Kanagy NL. Eucapnic intermittent hypoxia augments endothelin-1 vasoconstriction in rats: role of PKCdelta. Am J Physiol Heart Circ Physiol. 2008; 294:H920–H927. [PubMed: 18083893]
2. Bhat GB, Block ER. Effect of hypoxia on phospholipid metabolism in porcine pulmonary artery endothelial cells. Am J Physiol. 1992; 262:L606–L613. [PubMed: 1590410]
3. Broughton BR, Walker BR, Resta TC. Chronic hypoxia induces Rho kinase-dependent myogenic tone in small pulmonary arteries. Am J Physiol Lung Cell Mol Physiol. 2008; 294:L797–L806. [PubMed: 18263668]
4. Chen SJ, Chen YF, Meng QC, Durand J, DiCarlo VS, Oparil S. Endothelin-receptor antagonist bosentan prevents and reverses hypoxic pulmonary hypertension in rats. J Appl Physiol. 1995; 79:2122–2131. [PubMed: 8847282]
5. Deng Z, Morse JH, Slager SL, Cuervo N, Moore KJ, Venetos G, et al. Familial primary pulmonary hypertension (gene PPH1) is caused by mutations in the bone morphogenetic protein receptor-II gene. Am J Hum Genet. 2000; 67:737–744. [PubMed: 10903931]
6. Engebretsen BJ, Irwin D, Valdez ME, O'Donovan MK, Tucker A, van Patot MT. Acute hypobaric hypoxia (5486 m) induces greater pulmonary HIF-1 activation in Hilltop, compared to Madison, rats. High Alt Med Biol. 2007; 8:312–321. [PubMed: 18081507]
7. Flores I, Martinez A, Hannun YA, Merida I. Dual role of ceramide in the control of apoptosis following IL-2 withdrawal. J Immunol. 1998; 160:3528–3533. [PubMed: 9531315]
8. Golovina VA, Platoshyn O, Bailey CL, Wang J, Limsuwan A, Sweeney M, et al. Upregulated TRP and enhanced capacitative Ca(2+) entry in human pulmonary artery myocytes during proliferation. Am J Physiol Heart Circ Physiol. 2001; 280:H746–H755. [PubMed: 11158974]
9. Hofmann T, Obukhov AG, Schaefer M, Harteneck C, Gudermann T, Schultz G. Direct activation of human TRPC6 and TRPC3 channels by diacylglycerol. Nature. 1999; 397:259–263. [PubMed: 9930701]

10. Homma N, Nagaoka T, Morio Y, Ota H, Gebb SA, Karoor V, et al. Endothelin-1 and serotonin are involved in activation of RhoA/Rho kinase signaling in the chronically hypoxic hypertensive rat pulmonary circulation. J Cardiovasc Pharmacol. 2007; 50:697–702. [PubMed: 18091588]
11. Inoue R, Okada T, Onoue H, Hara Y, Shimizu S, Naitoh S, et al. The transient receptor potential protein homologue, TRP6, is the essential component of vascular alpha(1)-adrenoceptor-activated Ca(2+)-permeable cation channel. Circ Res. 2001; 88:325–332. [PubMed: 11179201]
12. Jernigan NL, Broughton BR, Walker BR, Resta TC. Impaired NO-dependent inhibition of store- and receptor-operated calcium entry in pulmonary vascular smooth muscle after chronic hypoxia. Am J Physiol Lung Cell Mol Physiol. 2006; 290:L517–L525. [PubMed: 16243900]
13. Jernigan NL, Walker BR, Resta TC. Chronic hypoxia augments protein kinase G-mediated Ca^{2+} desensitization in pulmonary vascular smooth muscle through inhibition of RhoA/Rho kinase signaling. Am J Physiol Lung Cell Mol Physiol. 2004; 287:L1220–L1229. [PubMed: 15310556]
14. Jernigan NL, Walker BR, Resta TC. Endothelium-derived reactive oxygen species and endothelin-1 attenuate NO-dependent pulmonary vasodilation following chronic hypoxia. Am J Physiol Lung Cell Mol Physiol. 2004; 287:L801–L808. [PubMed: 15180921]
15. Jernigan NL, Walker BR, Resta TC. Reactive oxygen species mediate RhoA/Rho kinase-induced Ca^{2+} sensitization in pulmonary vascular smooth muscle following chronic hypoxia. Am J Physiol Lung Cell Mol Physiol. 2008; 295:L515–L529. [PubMed: 18621909]
16. Kawanabe Y, Hashimoto N, Masaki T. Ca(2+) channels involved in endothelin-induced mitogenic response in carotid artery vascular smooth muscle cells. Am J Physiol Cell Physiol. 2002; 282:C330–C337. [PubMed: 11788344]
17. Kawanabe Y, Hashimoto N, Masaki T. Effects of phosphoinositide 3-kinase on endothelin-1-induced activation of voltage-independent Ca^{2+} channels and vasoconstriction. Biochem Pharmacol. 2004; 68:215–221. [PubMed: 15193993]
18. Keegan A, Morecroft I, Smillie D, Hicks MN, MacLean MR. Contribution of the 5-HT(1B) receptor to hypoxia-induced pulmonary hypertension: converging evidence using 5-HT(1B)-receptor knockout mice and the 5-HT(1B/1D)-receptor antagonist, GR127935. Circ Res. 2001; 89:1231–1239. [PubMed: 11739290]
19. Knot HJ, Nelson MT. Regulation of arterial diameter and wall [Ca^{2+}] in cerebral arteries of rat by membrane potential and intravascular pressure. J Physiol. 1998; 508(Pt 1):199–209. [PubMed: 9490839]
20. Kwan HY, Huang Y, Yao X. Protein kinase C can inhibit TRPC3 channels indirectly via stimulating protein kinase G. J Cell Physiol. 2006; 207:315–321. [PubMed: 16331690]
21. Langleben D, Jones RC, Aronovitz MJ, Hill NS, Ou LC, Reid LM. Pulmonary artery structural changes in two colonies of rats with different sensitivity to chronic hypoxia. Am J Pathol. 1987; 128:61–66. [PubMed: 3605313]
22. Lin MJ, Leung GP, Zhang WM, Yang XR, Yip KP, Tse CM, et al. Chronic hypoxia-induced upregulation of store- and receptor-operated Ca^{2+} channels in pulmonary arterial smooth muscle cells: a novel mechanism of hypoxic pulmonary hypertension. Circ Res. 2004; 95:496–505. [PubMed: 15256480]
23. Markou T, Yong CS, Sugden PH, Clerk A. Regulation of protein kinase C delta by phorbol ester, endothelin-1, and platelet-derived growth factor in cardiac myocytes. J Biol Chem. 2006; 281:8321–8331. [PubMed: 16361709]
24. Newman JH, Wheeler L, Lane KB, Loyd E, Gaddipati R, Phillips JA III, et al. Mutation in the gene for bone morphogenetic protein receptor II as a cause of primary pulmonary hypertension in a large kindred. NEJM. 2001; 345:319–324. [PubMed: 11484688]
25. Ng LC, Kyle BD, Lennox AR, Shen XM, Hatton WJ, Hume JR. Cell culture alters Ca^{2+} entry pathways activated by store-depletion or hypoxia in canine pulmonary arterial smooth muscle cells. Am J Physiol Cell Physiol. 2008; 294:C313–C323. [PubMed: 17977940]
26. Niermeyer S, Yang P, Shanmina, Drolkar, Zhuang J, Moore LG. Arterial oxygen saturation in Tibetan and Han infants born in Lhasa, Tibet. NEJM. 1995; 333:1248–1252. [PubMed: 7566001]
27. Nobe K, Miyatake M, Nobe H, Sakai Y, Takashima J, Momose K. Novel diacylglycerol kinase inhibitor selectively suppressed an U46619-induced enhancement of mouse portal vein contraction under high glucose conditions. Br J Pharmacol. 2004; 143:166–178. [PubMed: 15289283]

28. Ou LC, Sardella GL, Hill NS, Tenney SM. Acute and chronic pulmonary pressor responses to hypoxia: the role of blunting in acclimatization. Respir Physiol. 1986; 64:81–91. [PubMed: 3704382]
29. Platoshyn O, Yu Y, Golovina VA, McDaniel SS, Krick S, Li L, et al. Chronic hypoxia decreases K(V) channel expression and function in pulmonary artery myocytes. Am J Physiol Lung Cell Mol Physiol. 2001; 280:L801–L812. [PubMed: 11238022]
30. Resta TC, Chicoine LG, Omdahl JL, Walker BR. Maintained upregulation of pulmonary eNOS gene and protein expression during recovery from chronic hypoxia. Am J Physiol. 1999; 276:H699–H708. [PubMed: 9950873]
31. Resta TC, Walker BR. Orally administered L-arginine does not alter right ventricular hypertrophy in chronically hypoxic rats. Am J Physiol. 1994; 266:R559–R563. [PubMed: 8141415]
32. Resta TC, Walker BR. Chronic hypoxia selectively augments endothelium-dependent pulmonary arterial vasodilation. Am J Physiol. 1996; 270:H888–H896. [PubMed: 8780183]
33. Sage SO, Reast R, Rink TJ. ADP evokes biphasic Ca^{2+} influx in fura-2-loaded human platelets. Evidence for Ca^{2+} entry regulated by the intracellular Ca^{2+} store. Biochem J. 1990; 265:675–680. [PubMed: 2306207]
34. Severson DL, Hee-Cheong M. Diacylglycerol metabolism in isolated aortic smooth muscle cells. Am J Physiol. 1989; 256:C11–C17. [PubMed: 2536225]
35. Shimoda LA, Sham JS, Shimoda TH, Sylvester JT. L-type Ca(2+) channels, resting [Ca(2+)](i), and ET-1-induced responses in chronically hypoxic pulmonary myocytes. Am J Physiol Lung Cell Mol Physiol. 2000; 279:L884–L894. [PubMed: 11053024]
36. Shimoda LA, Sylvester JT, Sham JS. Mobilization of intracellular Ca(2+) by endothelin-1 in rat intrapulmonary arterial smooth muscle cells. Am J Physiol Lung Cell Mol Physiol. 2000; 278:L157–L164. [PubMed: 10645903]
37. Sweeney M, McDaniel SS, Platoshyn O, Zhang S, Yu Y, Lapp BR, et al. Role of capacitative Ca^{2+} entry in bronchial contraction and remodeling. J Appl Physiol. 2002; 92:1594–1602. [PubMed: 11896026]
38. Temes E, Martin-Puig S, Aragones J, Jones DR, Olmos G, Merida I, et al. Role of diacylglycerol induced by hypoxia in the regulation of HIF-1alpha activity. Biochem Biophys Res Commun. 2004; 315:44–50. [PubMed: 15013423]
39. Venkatachalam K, Zheng F, Gill DL. Regulation of canonical transient receptor potential (TRPC) channel function by diacylglycerol and protein kinase C. J Biol Chem. 2003; 278:29031–29040. [PubMed: 12721302]
40. Wang J, Shimoda LA, Sylvester JT. Capacitative calcium entry and TRPC channel proteins are expressed in rat distal pulmonary arterial smooth muscle. Am J Physiol Lung Cell Mol Physiol. 2004; 286:L848–L858. [PubMed: 14672922]
41. Wang J, Weigand L, Lu W, Sylvester JT, Semenza GL, Shimoda LA. Hypoxia inducible factor 1 mediates hypoxia-induced TRPC expression and elevated intracellular Ca^{2+} in pulmonary arterial smooth muscle cells. Circ Res. 2006; 98:1528–1537. [PubMed: 16709899]
42. Wang J, Weigand L, Wang W, Sylvester JT, Shimoda LA. Chronic hypoxia inhibits Kv channel gene expression in rat distal pulmonary artery. Am J Physiol Lung Cell Mol Physiol. 2005; 288:L1049–L1058. [PubMed: 15665041]
43. Yang T, Roder KE, Bhat GJ, Thekkumkara TJ, Abbruscato TJ. Protein kinase C family members as a target for regulation of blood-brain barrier Na, K,2Cl-cotransporter during in vitro stroke conditions and nicotine exposure. Pharm Res. 2006; 23:291–302. [PubMed: 16450214]
44. Yu Y, Fantozzi I, Remillard CV, Landsberg JW, Kunichika N, Platoshyn O, et al. Enhanced expression of transient receptor potential channels in idiopathic pulmonary arterial hypertension. Proc Natl Acad Sci U S A. 2004; 101:13861–13866. [PubMed: 15358862]
45. Yuan JX, Aldinger AM, Juhaszova M, Wang J, Conte JV Jr, Gaine SP, et al. Dysfunctional voltage-gated K^{+} channels in pulmonary artery smooth muscle cells of patients with primary pulmonary hypertension. Circulation. 1998; 98:1400–1406. [PubMed: 9760294]
46. Zhang S, Dong H, Rubin LJ, Yuan JX. Upregulation of Na^{+}/Ca^{2+} exchanger contributes to the enhanced Ca^{2+} entry in pulmonary artery smooth muscle cells from patients with idiopathic

pulmonary arterial hypertension. Am J Physiol Cell Physiol. 2007; 292:C2297–C2305. [PubMed: 17192285]

47. Zhang S, Patel HH, Murray F, Remillard CV, Schach C, Thistlethwaite PA, et al. Pulmonary artery smooth muscle cells from normal subjects and IPAH patients show divergent cAMP-mediated effects on TRPC expression and capacitative Ca^{2+} entry. Am J Physiol Lung Cell Mol Physiol. 2007; 292:L1202–L1210. [PubMed: 17189322]
48. Zhang XF, Iwamuro Y, Enoki T, Okazawa M, Lee K, Komuro T, et al. Pharmacological characterization of Ca^{2+} entry channels in endothelin-1-induced contraction of rat aorta using LOE 908 and SK&F 96365. Br J Pharmacol. 1999; 127:1388–1398. [PubMed: 10455288]
49. Zhao L, Sebkhi A, Nunez DJ, Long L, Haley CS, Szpirer J, et al. Right ventricular hypertrophy secondary to pulmonary hypertension is linked to rat chromosome 17: evaluation of cardiac ryanodine Ryr2 receptor as a candidate. Circulation. 2001; 103:442–447. [PubMed: 11157698]
50. Zhu MH, Chae M, Kim HJ, Lee YM, Kim MJ, Jin NG, et al. Desensitization of canonical transient receptor potential channel 5 by protein kinase C. Am J Physiol Cell Physiol. 2005; 289:C591–C600. [PubMed: 15843439]

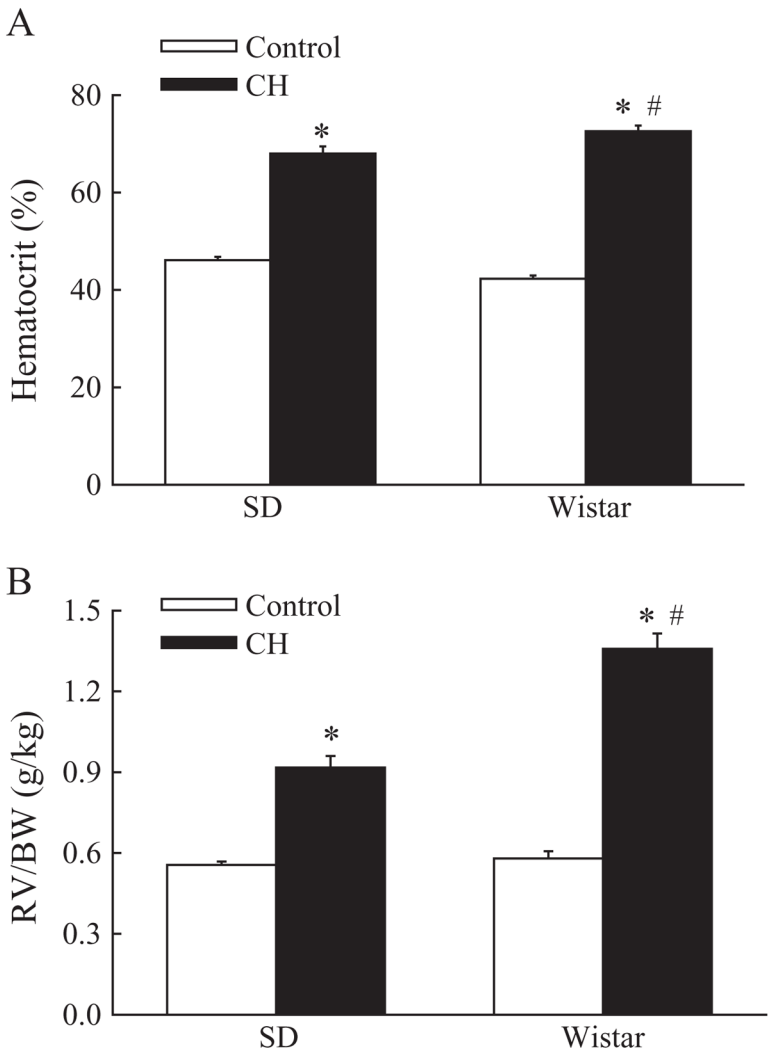

Figure 1.

(A) Chronic hypoxia (CH) elicits a greater polycythemic response (percent hematocrit) in Wistar, compared to Sprague-Dawley (SD), rats. Values are means±standard error (SE) of n=7–11 rats/group. $^{*}P$<0.05 vs. corresponding control group; $^{\#}P$<0.05 vs. SD. (B) CH induces greater right ventricular hypertrophy [ratio of right ventricle (RV) to body weight (BW)] in Wistar vs. SD rats. Values are means±SE of n=7–11 rats/group. $^{*}P$<0.05 vs. corresponding control group; $^{\#}P$<0.05 vs. SD.

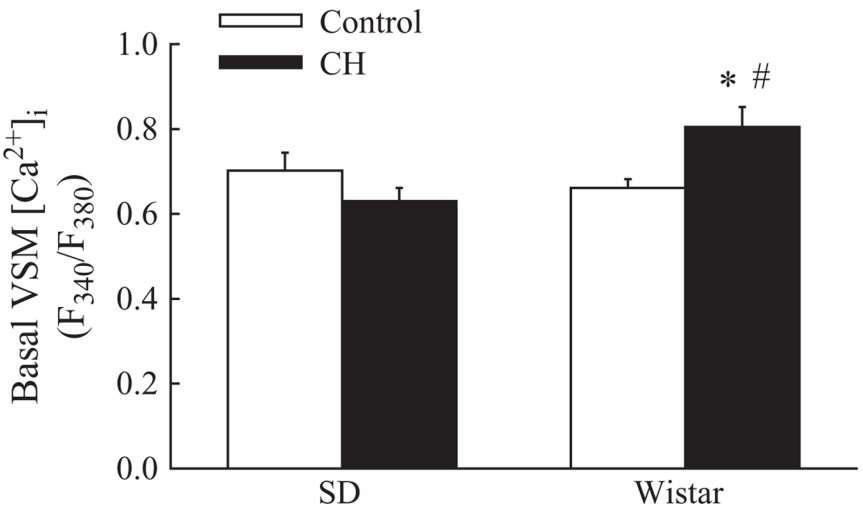

Figure 2.

CH increases basal pulmonary vascular smooth muscle (VSM) intracellular free calcium concentration ($[Ca^{2+}]_i$) in Wistar, but not SD, rats. $[Ca^{2+}]_i$ is expressed as the ratio of fluorescence emitted following excitation at 340 and 380 nm (F_{340}/F_{380}) in pressurized, endothelium-disrupted pulmonary arteries. Values are means±standard error of n=9–17 arteries/group. $^{*}P< 0.05$ vs. corresponding control group; $^{\#}P<0.05$ vs. SD.

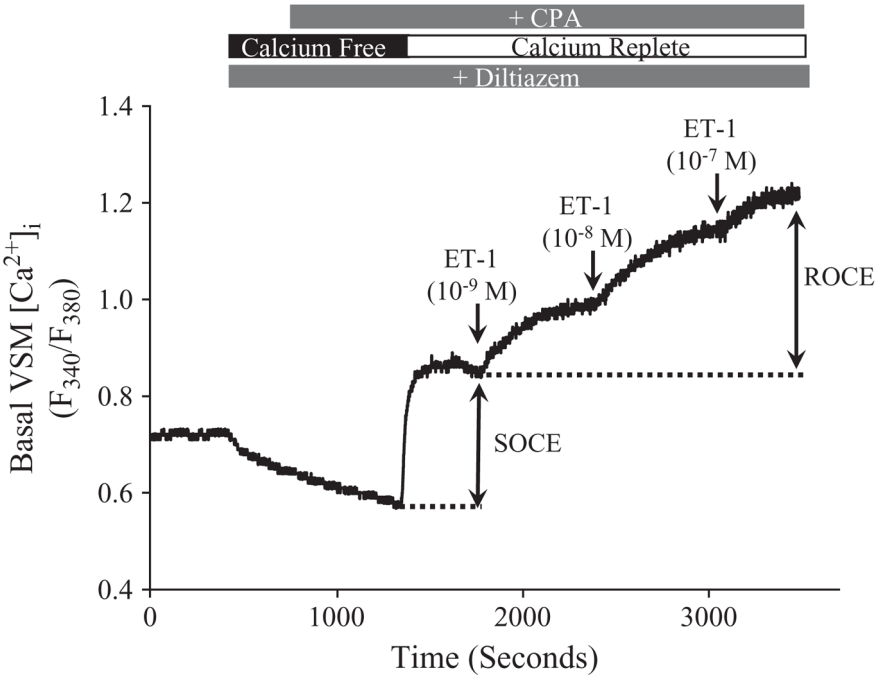

Figure 3.

Representative trace of VSM $[Ca^{2+}]_i$ (F_{340}/F_{380}) in an endothelium-disrupted control artery demonstrating store-operated Ca^{2+} entry (SOCE) and endothe-lin-1 (ET-1)-induced receptor-operated Ca^{2+} entry (ROCE). The SERCA inhibitor, cyclopiazonic acid (CPA; 10 μM), was used to deplete intracellular Ca^{2+} stores and thereby activate store-operated cation channels. SOCE was then assessed following the restoration of extracellular Ca^{2+}. ET-1 (1–100 nM) was added to elicit ROCE subsequent to a generation of a stable SOCE response. All experiments were conducted in the presence of diltiazem (50 μM) to inhibit L-type voltage-gated Ca^{2+} channels.

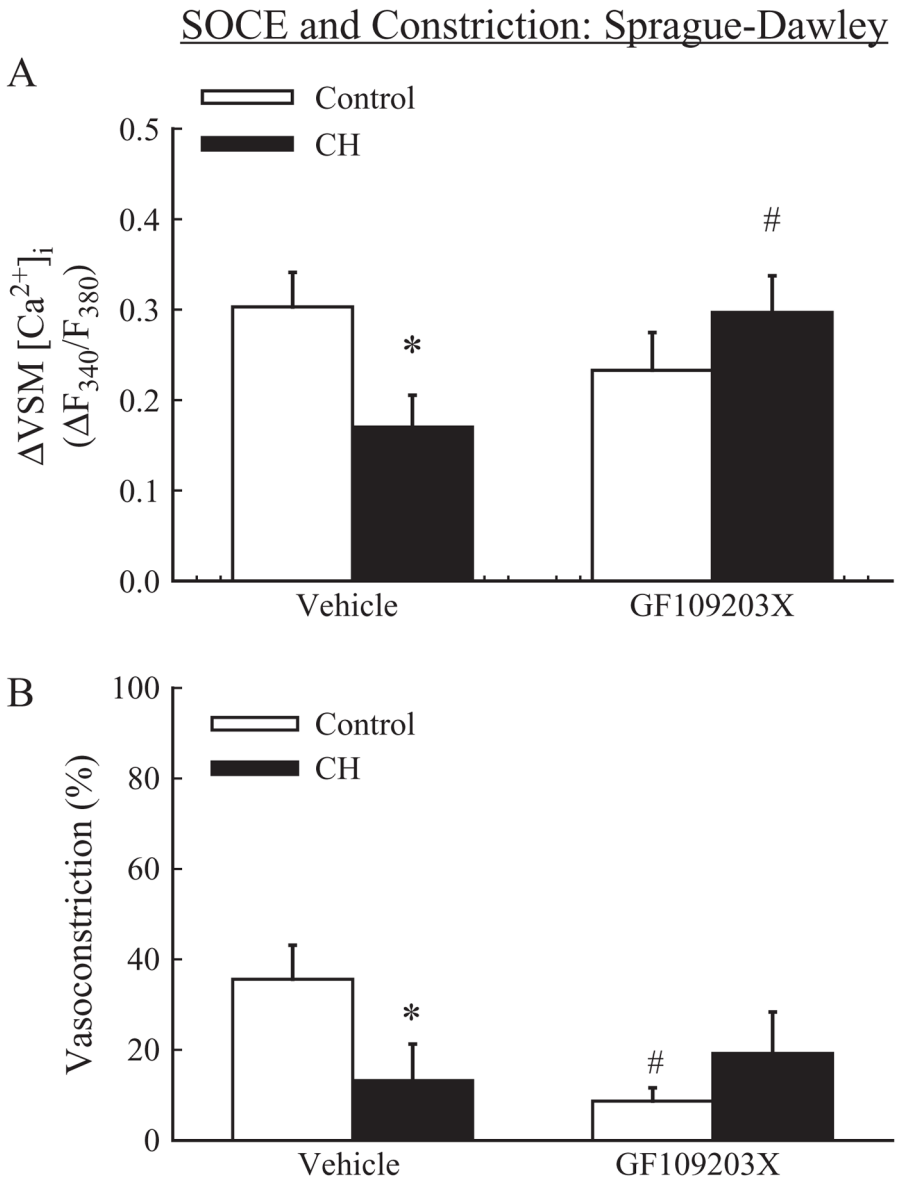

Figure 4.

SOCE in Sprague-Dawley rats: CH attenuates SOCE through a PKC-dependent mechanism. (A) SOCE expressed as a change (Δ) in F_{340}/F_{380} in endothelium-disrupted pulmonary arteries from control and CH Sprague-Dawley rats in the presence of vehicle or GF109203X (1 μM) and (B) associated vasoconstriction expressed as a percent of basal inner diameter. Experiments were performed in the presence of CPA and diltiazem. Values are means ±standard error of n=6–7 rats/group. $^{*}P<0.05$ vs. respective control group; $^{\#}P< 0.05$ vs. vehicle.

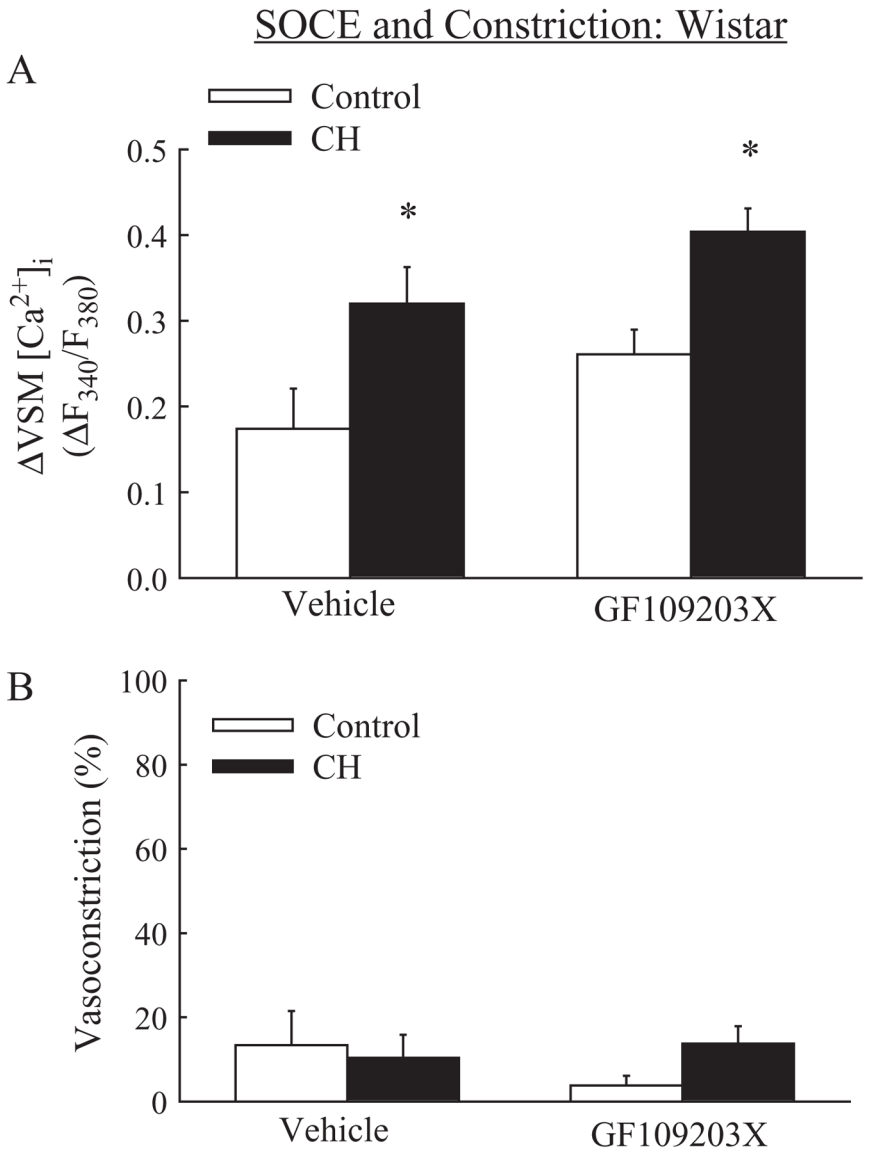

Figure 5.

SOCE in Wistar rats: augmented SOCE following CH is independent of PKC. (A) SOCE in arteries from control and CH Wistar rats in the presence of vehicle or GF109203X and (B) associated vasoconstriction. Experiments were performed in the presence of cyclopiazonic acid and diltiazem. Values are means±standard error of n=8–9 rats/group. $^{*}P<0.05$ vs. respective control group.

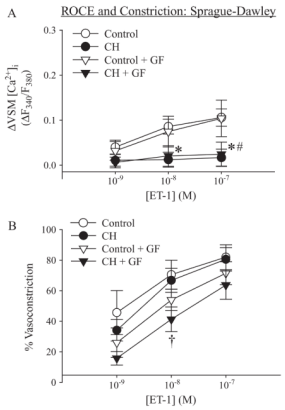

Figure 6.

ROCE in Sprague-Dawley rats: Chronic hypoxia (CH) decreases ET-1-induced ROCE via a PKC-independent signaling pathway. (A) ET-1 (1–100 nM)-induced ROCE in arteries from control and CH Sprague-Dawley rats in the presence of vehicle or GF109203X (GF; 1 μM) and (B) associated vasoconstriction expressed as a percent of inner diameter at the plateau of the SOCE-induced vasoconstriction. Experiments were performed in the presence of CPA and diltiazem. Values are means±standard error of n=6–7 rats/group. $^{*}P<0.05$ control vehicle vs. CH vehicle; $^{\#}P<0.05$ control GF vs. CH GF; $^{\dagger}P<0.05$ CH vehicle vs. CH GF.

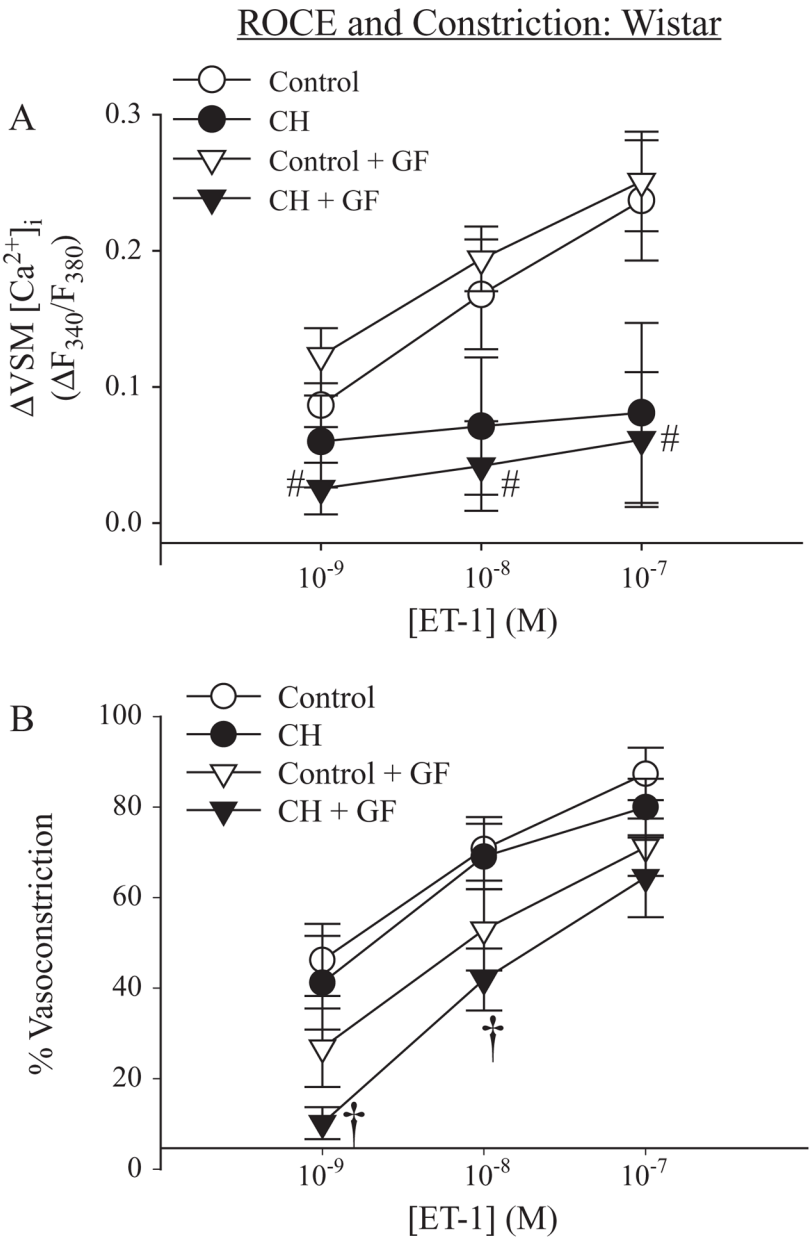

Figure 7.

ROCE in Wistar rats: ET-1-induced ROCE is mediated by a PKC-independent signaling mechanism. (A) ET-1-induced ROCE in arteries from control and CH Wistar rats in the presence of vehicle and GF109203X (GF) and (B) associated vasoconstriction. Experiments were performed in the presence of CPA and diltiazem. Values are means±standard error of n=6–7 rats/group. $^{\#}P<0.05$ control GF vs. CH GF. $^{\dagger}P<0.05$ CH vehicle vs. CH GF.

Table 1

Heart and Body-Weight Data.

	RV/T (g/g)	LV+S/BW (g/kg)	BW (kg)	*n*
Control Sprague-Dawley	0.199 ± 0.004	2.24 ± 0.02	0.277±0.005	11
CH Sprague-Dawley	0.300 ± 0.009*	2.15 ± 0.04	0.325±0.007	10
Control Wistar	0.219 ± 0.006#	2.06 ± 0.03	0.337±0.016#	8
CH Wistar	0.325 ± 0.006*,#	2.84 ± 0.16*,#	0.319±0.005*	8

Values are means ± standard error. *n*, number of rats.

*$P<0.05$ vs. respective control;

#$P<0.05$ vs. Sprague-Dawley.

Table 2

In Situ Fura-2 Calibration Values.

	Low calibration (F_{340}/F_{380})	High calibration (F_{340}/F_{380})	*n*
Control Sprague-Dawley	0.52 ± 0.04	1.68 ± 0.18	4
CH Sprague-Dawley	0.47 ± 0.01	1.72 ± 0.06	3
Control Wistar	0.56 ± 0.02	1.99 ± 0.15	4
CH Wistar	0.57 ± 0.06	1.94 ± 0.09	4

Values are means ± standard error. *n*, number of rats. There are no significant differences.

Table 3

Basal Arterial Intralumenal Diameter.

	Inner diameter (μm)	*n*
Control Sprague-Dawley	166 ± 13	13
CH Sprague-Dawley	125 ± 11*	14
Control Wistar	145 ± 11	14
CH Wistar	135 ± 8	15

Values are means±standard error. *n*, number of rats.

*$P<0.05$ vs. control.